Earth and Planetary Science Letters 498 (2018) 348–361

Contents lists available at ScienceDirect

Earth and Planetary Science Letters

www.elsevier.com/locate/epsl

Early Cretaceous origin of the Woyla Arc (Sumatra, Indonesia) on the Australian plate

Eldert L. Advokaat [a,*], Mayke L.M. Bongers [a], Alfend Rudyawan [b], Marcelle K. BouDagher-Fadel [c], Cor G. Langereis [a], Douwe J.J. van Hinsbergen [a]

[a] Department of Earth Sciences, Utrecht University, 3584 CS Utrecht, the Netherlands
[b] Geology Study Program, Institut Teknologi Bandung, Bandung, Jawa Barat 40132, Indonesia
[c] Department of Earth Sciences, University College London, London WC1E 6BT, United Kingdom

A R T I C L E I N F O

Article history:
Received 14 March 2018
Received in revised form 25 June 2018
Accepted 1 July 2018
Available online 20 July 2018
Editor: A. Yin

Keywords:
Woyla Arc
intra-oceanic arc
paleomagnetism
plate tectonics
Sundaland
Sumatra

A B S T R A C T

Key to understanding the plate kinematic evolution of the Neotethys oceanic domain that existed between the Gondwana-derived Indian and Australian continents in the south, and Eurasia in the north, is the reconstruction of oceanic plates that are now entirely lost to subduction. Relics of these oceanic plates exist in the form of ophiolites and island arcs accreted to the orogen that stretches from Tibet and the Himalayas to SE Asia that formed the southern margin of Sundaland. The intra-oceanic Woyla Arc thrusted over western Sundaland – the Eurasian core of SE Asia – in the mid-Cretaceous. The Woyla Arc was previously interpreted to have formed above a west-dipping subduction zone in the Early Cretaceous, synchronous with east-dipping subduction below Sundaland. The oceanic 'Ngalau Plate' between the Woyla Arc and Sundaland was lost to subduction. We present paleomagnetic results from Lower Cretaceous limestones and volcaniclastic rocks of the Woyla Arc, Middle Jurassic radiolarian cherts of the intervening Ngalau Plate, and Upper Jurassic–Lower Cretaceous detrital sediments of the Sundaland margin. Our results suggest that the Woyla Arc was formed around equatorial latitudes and only underwent an eastward longitudinal motion relative to Sundaland. This is consistent with a scenario where the Woyla Arc was formed on the edge of the Australian plate. We propose a reconstruction where the Ngalau Plate formed a triangular oceanic basin between the N–S trending Woyla Arc and the NW-SE trending Sundaland margin to account for the absence of accreted arc rocks in the Himalayas. As consequence of this triangular geometry, accretion of the Woyla Arc to the western Sundaland margin was diachronous, accommodated by a southward migrating triple junction. Continuing convergence of the Australia relative to Eurasia was accommodated by subduction polarity reversal behind the Woyla Arc, possibly recorded by Cretaceous ophiolites in the Indo-Burman Ranges and the Andaman-Nicobar Islands.

1. Introduction

Plate kinematic reconstructions are first and foremost based on marine magnetic anomalies and fracture zones of the modern oceans, aided by geologic and paleomagnetic data from the stable continents (Seton et al., 2012; e.g. Torsvik et al., 2012). Quantifying the motions of former oceanic plates and their intra-oceanic boundaries that were subsequently lost to subduction, however, is notoriously difficult, and the resolution of plate kinematic restorations thus decreases back in time. If such former intra-oceanic plate boundaries were subduction zones, relics may be available in the geologic record in the form of accreted and deformed island arcs and ophiolites that may allow constraining intra-oceanic plate boundary evolution in deep geologic time.

The vast Neotethys oceanic domain existed between the Australian and Indian continents in the south, and Eurasia in the north. Convergence and collision between these continents and the plates that hosted them led to the formation and complex deformation of the orogen that stretches from Tibet and the Himalaya in the northwest to SE Asia in the southeast (Fig. 1) and little is known about the plates that may have existed within the Neotethys ocean that have now been subducted.

In the central part of this orogen, on the island of Sumatra, lies the accreted Upper Jurassic–Lower Cretaceous Woyla Arc which may shed light on the past intra-oceanic plate configurations (Fig. 1). This arc is interpreted as a former intra-oceanic

* Corresponding author.
E-mail address: E.L.Advokaat@uu.nl (E.L. Advokaat).

https://doi.org/10.1016/j.epsl.2018.07.001

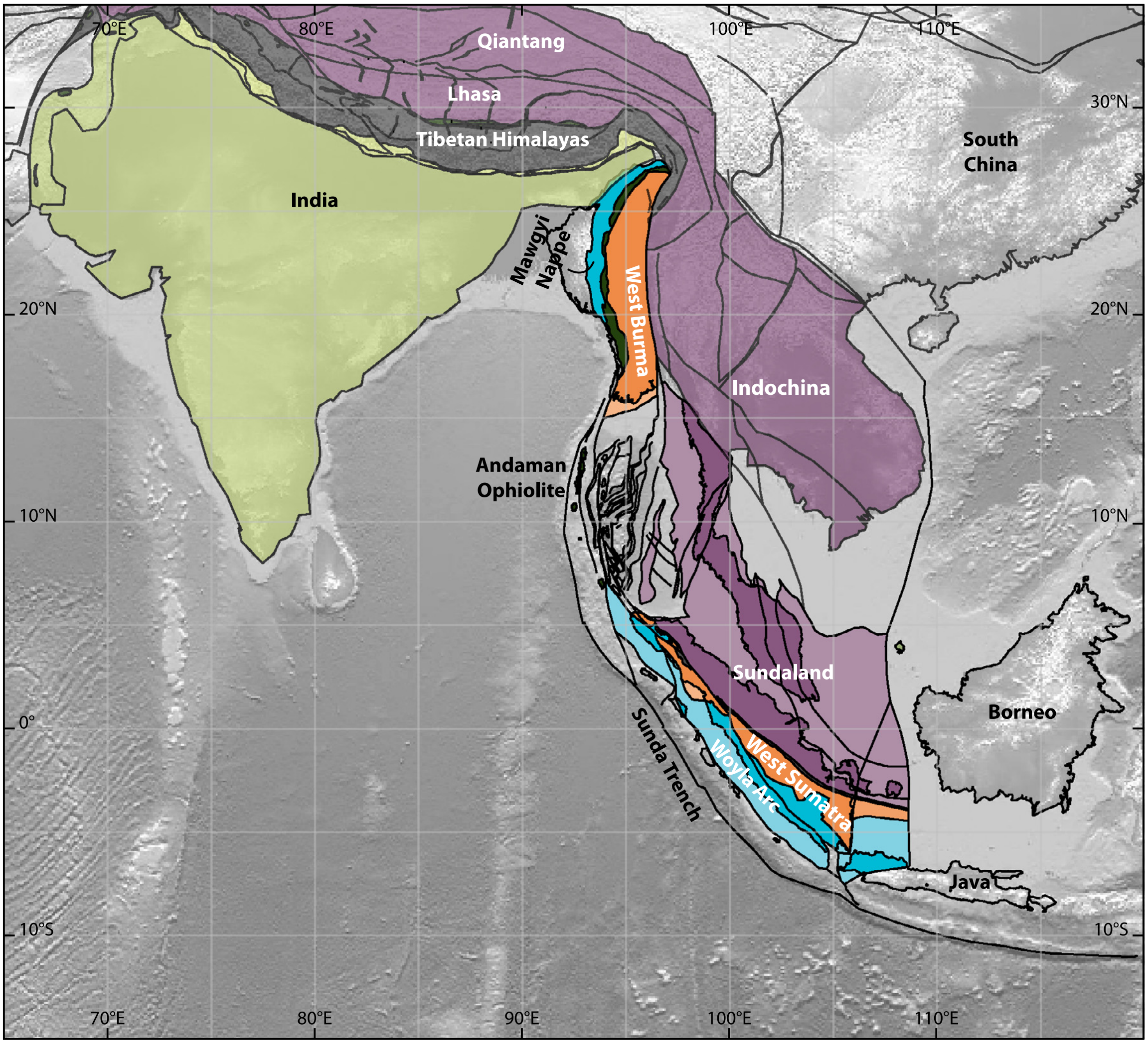

Fig. 1. Map of continental and arc fragments in SE Asia, modified from Barber et al. (2005), Metcalfe (2013), and van Hinsbergen et al. (2011) and Li et al. (2017).

subduction-related arc that lies thrust onto the continental West Sumatra Block in the mid-Cretaceous (e.g. Barber, 2000; Barber et al., 2005; Wajzer et al., 1991). The West Sumatra Block is thought to have been part of the Eurasian core of SE Asia – Sundaland – since the Late Triassic–Early Jurassic (Barber et al., 2005; Barber and Crow, 2009; Metcalfe, 2013, 1996). Because the continental margin of Sundaland hosts arc magmatic rocks of the same time interval as the Woyla Arc, Barber et al. (2005) suggested that the Woyla Arc was associated with a subduction plate boundary that was not the Eurasian plate boundary. From this it follows that at least one – presumably oceanic – plate must have existed within the eastern Neotethys surrounded by Eurasia, Australia, and possibly India (e.g. Hall, 2012).

In this study, we attempt at a kinematic reconstruction of this plate. To this end, we collected new paleomagnetic data from Upper Jurassic–Lower Cretaceous clastic sediments of West Sumatra and from volcaniclastics and limestones of the Woyla Arc. We use these to first test whether the West Sumatra Block was part of Sundaland. We then develop simplest-case plate kinematic scenarios in which the Woyla arc is assumed to have been part of the Indian, Australian, or Tethyan Himalayan plates based on previous reconstructions (Seton et al., 2012; van Hinsbergen et al., 2018), placed in a paleomagnetic reference frame (Torsvik et al., 2012), and test these against our new paleomagnetic data. Finally, we provide a plate kinematic scenario for the eastern Neotethys that may explain the origin and arrest of the Woyla Arc, and the formation of the modern plate boundary along western and southern Sundaland.

2. Geologic setting

Sundaland is the core of SE Asia and consists of multiple continental blocks and volcanic arcs, bounded by suture zones representing remnants of closed ocean basins (e.g. Hall, 2012; Metcalfe, 2013, 1996). The core of Sundaland consists of the Indochina-East Malaya, Sibumasu, West-Sumatra, West Burma, and SW Borneo blocks that amalgamated against the South China Block in the north during the Paleozoic to Late Mesozoic (e.g. Hall, 2012; Metcalfe, 2013, 1996). The continental terranes are thought to have separated from the northern margin of eastern Gondwana, opening new oceans to their south and closing older ones to their north upon their northward flight towards Sundaland (e.g. Metcalfe, 2013, 1996). The Woyla Arc in Sumatra is the latest major crustal block that accrete to Sundaland in the Late Cretaceous (e.g. Barber, 2000; Hall, 2012; Metcalfe, 2013, 1996) (Fig. 1). Rocks of the Mawgyi Nappe were accreted to the West Burma Block to the north, which was in pre-Neogene time likely 500–1000 km farther south than today relative to Sumatra (e.g. Mitchell, 1993 and references therein; van Hinsbergen et al., 2011), have been suggested as equivalents to the Woyla Arc (Barber and Crow, 2009; Mitchell, 1993). Hall (2012) interpreted the Woyla arc to be contiguous with an intra-oceanic subduction zone (Incertus Arc) that

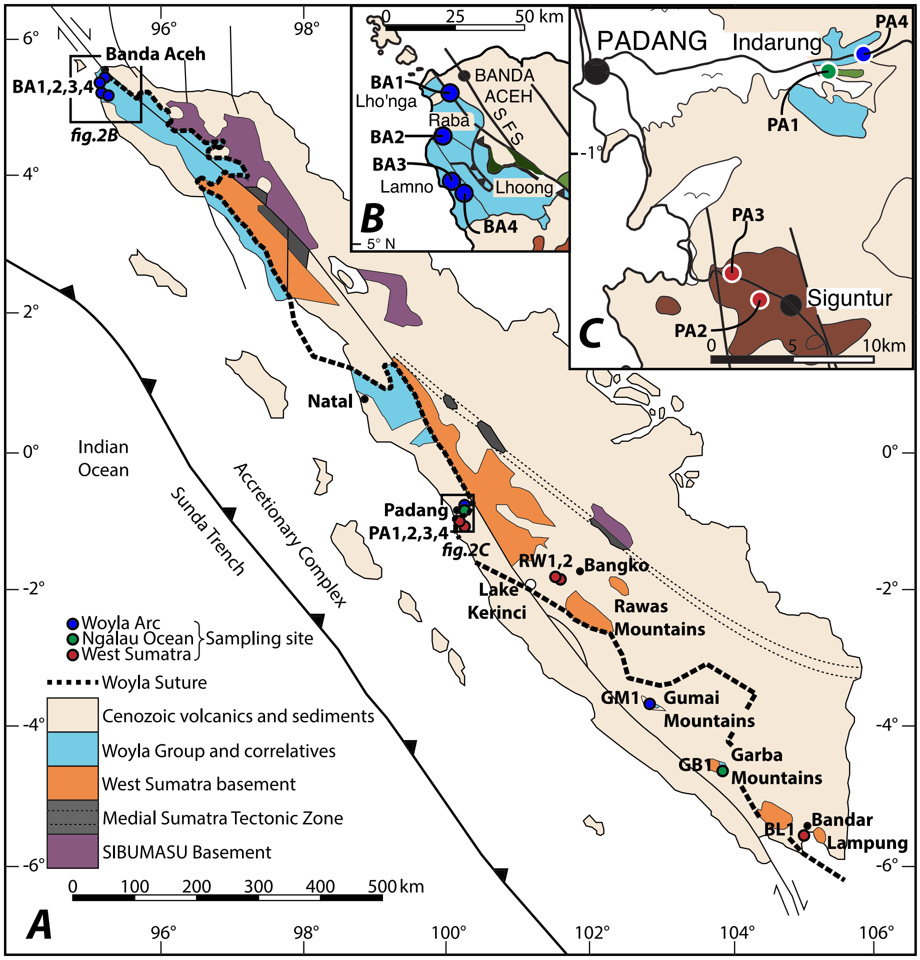

Fig. 2. A) Simplified geological map of Sumatra and sample locations, B) Detail map of Aceh, C) Detail map of Padang, modified from Barber (2000) and Barber et al. (2005). (For interpretation of the colours in the figure(s), the reader is referred to the web version of this article.)

would include the Lower Cretaceous ophiolites found in the Indus-Yarlung suture of southern Tibet. These ophiolites have previously been interpreted to have formed at the equator (Abrajevitch et al., 2005), which would support such a scenario. Recent paleomagnetic and sediment provenance data from the Indus-Yarlung ophiolites, however, demonstrated that these formed in the forearc of southern Tibet at a latitude of ∼16°N and that previous low-latitude interpretations were likely an artefact from unrecognised compaction-induced inclination shallowing (Huang et al., 2015b). No accreted Lower Cretaceous arc rocks that may be equivalent to the Woyla Arc are known from the accretionary prisms below the Tibetan ophiolites, and there is no evidence that the Woyla arc continues to the longitude of Tibet.

The present-day margin of Sundaland in the Sumatra region is characterised by oblique subduction of the Indian–Australian plate accommodated by the Sunda trench (Fig. 2a). In the Pliocene–Pleistocene this oblique subduction became partitioned over the trench and the right-lateral Sumatran Fault System (SFS) that cuts through all rock units along the strike of Sumatra and has an estimated displacement of 50–150 km (Barber, 2000; Barber et al., 2005). The geology of Sumatra is dominated by a Cenozoic volcanic arc, with active volcanoes built on pre-Cenozoic basement (Fig. 3). This basement is mainly exposed in the Barisan Mountains along the SFS (Barber, 2000).

The pre-Cenozoic basement of Sumatra is divided into four units: The East Sumatra Block which is part of Sibumasu, the Medial Sumatra Tectonic Zone that separates Sibumasu from the West Sumatra block, and the Upper Jurassic–Lower Cretaceous Woyla Group (Fig. 2a) (Cameron et al., 1980). The Woyla Group and correlatives comprise rocks of the Woyla Arc, an oceanic accretionary assemblage, and a continental-arc assemblage (Barber, 2000; Cameron et al., 1980). The Woyla Group is found in northern Sumatra near Banda Aceh and Natal, and similar units to the southeast with the same lithologies and age ranges, including near Padang, in the Gumai and Garba Mountains, and near Bandar Lampung are correlated with it (Fig. 2) (Barber, 2000). The Woyla Group is folded, presumably related to the collision of the Woyla Arc with the West Sumatra Block sometime in the mid-Cretaceous (Barber, 2000).

The Woyla volcanic arc assemblage consists mainly of basaltic to andesitic volcanic rocks that include xenoliths of radiolarian chert, dykes, and volcaniclastic sandstones lacking quartz, and shales (Barber, 2000; Wajzer et al., 1991). Sparse radiometric dating of the volcanic rocks yielded K–Ar ages of 122–105 Ma (Gafoer et al., 1992; Koning, 1985). In addition, Upper Jurassic–Lower Cretaceous limestones with volcanic detritus associated with the basaltic to andesitic volcanic rocks (Bennett et al., 1981; Gafoer et al., 1992; Yancey and Alif, 1977) are interpreted as fringing reefs built on volcanic edifices (Barber, 2000; Cameron et al., 1980; Wajzer et al., 1991). The volcanic arc assemblage and interlayered sedimentary rocks are nowhere associated with continent-derived rocks and are thus interpreted as remnants of a Late Jurassic - Early Cretaceous, intra-oceanic volcanic arc (Barber et al., 2005). The only previous paleomagnetic study on limestones of the Woyla Group was performed by Haile (1979), who reported a paleolatitude of 26°S, but also indicated that these rocks were remagne-

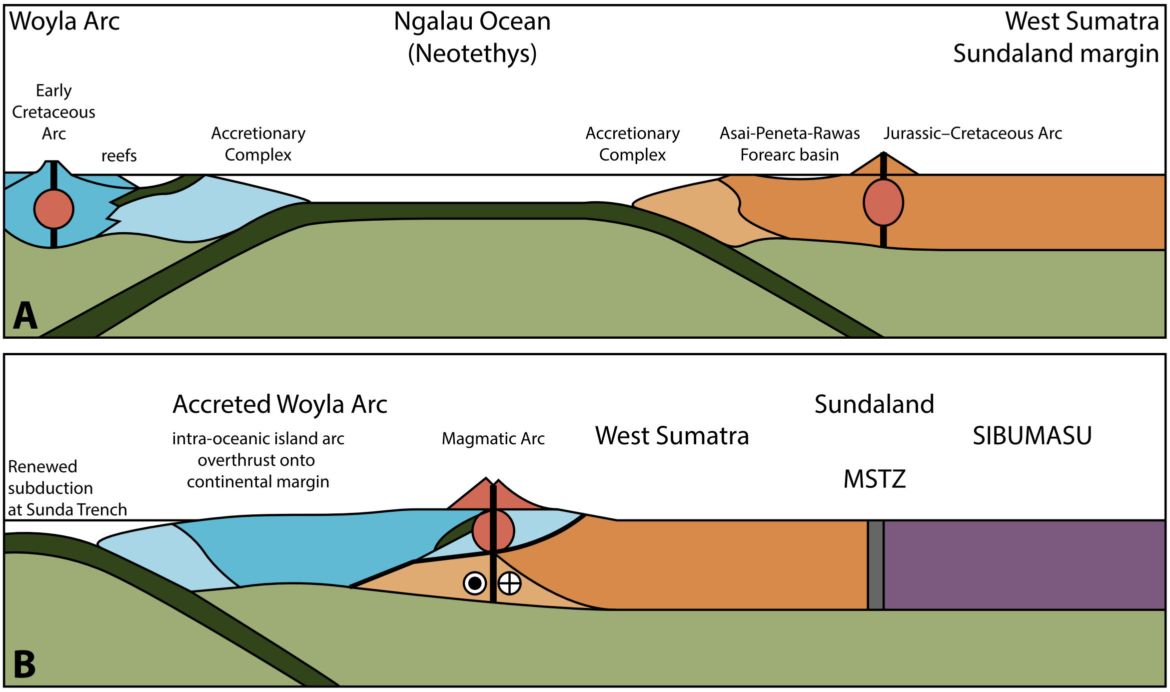

Fig. 3. Cross sections of the Woyla Arc and West Sumatra continental margin, modified from Barber et al. (2005). A) Early Cretaceous, B) mid-Cretaceous to present-day.

tised. Taking these data at face value, Metcalfe (1996) interpreted that the Woyla Arc originated near the northern margin of Eastern Gondwana in the southern hemisphere.

The oceanic accretionary assemblage contains internally deformed serpentinites, pillow basalts, cherts, volcanic breccia, gabbros and red shales separated by faults. This assemblage is interpreted as imbricated units derived from now-subducted ocean floor (Barber, 2000).

The continental-arc assemblage consists of Middle Jurassic–Lower Cretaceous quartzitic and calcareous sandstones and shales, intruded by Jurassic–Cretaceous granites. This assemblage is partially metamorphosed, with metamorphic grades increasing westwards up to amphibolite grade conditions (Suwarna et al., 1994). Metamorphic rocks yielded K–Ar ages of 125–95 Ma (Andi Mangga et al., 1994; Koning, 1985). This assemblage is interpreted to have formed at a subduction zone along the continental West Sumatra margin (Barber, 2000).

To account for synchronous magmatism at the intra-oceanic Woyla Arc and the West Sumatra active continental margin, and the juxtaposition of unmetamorphosed units of the Woyla Arc to metamorphosed units of the West Sumatra margin, Barber et al. (2005) suggested that the Woyla Arc formed above a SW-dipping (in modern coordinates) subduction zone, and the West Sumatra arc above a synchronous NE-dipping subduction zone. Upon mid-Cretaceous closure of the intervening oceanic lithosphere, the Woyla Arc was thrust over the West Sumatra margin (Barber et al., 2005) (Fig. 3).

3. Methods

3.1. Paleomagnetism

Rock samples from sedimentary rocks of the Woyla Group were obtained from 13 sites (Fig. 2, Table 1) using a petrol-powered drill with a drill bit having an inside diameter of 25 mm. We sampled intervals varying between 2 m to 70 m per site, enough to average out paleosecular variation (see parameter Table 1 and explanation below). Typically one core sample was collected per exposed bed. The cores were oriented in the field using a Brunton magnetic compass with an inclinometer attached. In cases where hand specimens were taken, cores were drilled normal to the orientation plane. The cores were cut into subsamples of 22 mm length using a double-blade circular saw.

Laboratory analyses were performed at the paleomagnetic laboratory Fort Hoofddijk at Utrecht University, The Netherlands. The natural remanent magnetisation (NRM) of samples was measured on a 2G DC-SQUID magnetometer and further investigated using thermal as well as alternating field (AF) stepwise demagnetisation. Stepwise thermal demagnetisation was carried out using 20–100 °C increment up to 660 °C (or until complete demagnetisation). Samples analysed by AF demagnetisation were heated to 150°C to remove goethite or possible stress induced by weathering (Velzen and Zijderveld, 1995), and then subjected to the following field strengths (in mT): 0, 4, 8, 12, 16, 20, 25, 30, 35, 40, 45, 50, 60, 70, (80, 90, 100).

Statistical analysis and interpretation were performed using the online, platform independent portal Paleomagnetism.org (Koymans et al., 2016). Demagnetisation diagrams are plotted as orthogonal vector diagrams (Zijderveld, 1967). Interpretation of demagnetisation diagrams was performed by interpreting a characteristic remanent magnetisation (ChRM) for components decaying towards the origin following an eigen vector approach (Kirschvink, 1980). We applied a 45° cut-off to the virtual geomagnetic pole (VGP) distribution of a set of directions (Deenen et al., 2011; following Johnson et al., 2008). This is an arbitrary fixed angle cut-off meant to remove outliers due to excursions or transitional directions, or to remove outliers due to (assumed, possible) errors in sampling, orientation or measurement. Mean directions were determined using Fisher (1953) statistics while directional statistics were derived from the corresponding VGP distribution (Deenen et al., 2011), and errors in declination (ΔD_x) and inclination (ΔI_x) were calculated from the cone of confidence ($A95$) of the mean VGP following Butler (Butler, 1992). We applied the reliability criteria of Deenen et al. (2011) by determining $A95$ of the VGP distribution, and calculate the N-dependent values of $A95_{min}$ and $A95_{max}$. Values plotting within this envelope may be straightforwardly explained by paleosecular variation (PSV). Values of $A95 > A95_{max}$ may indicate

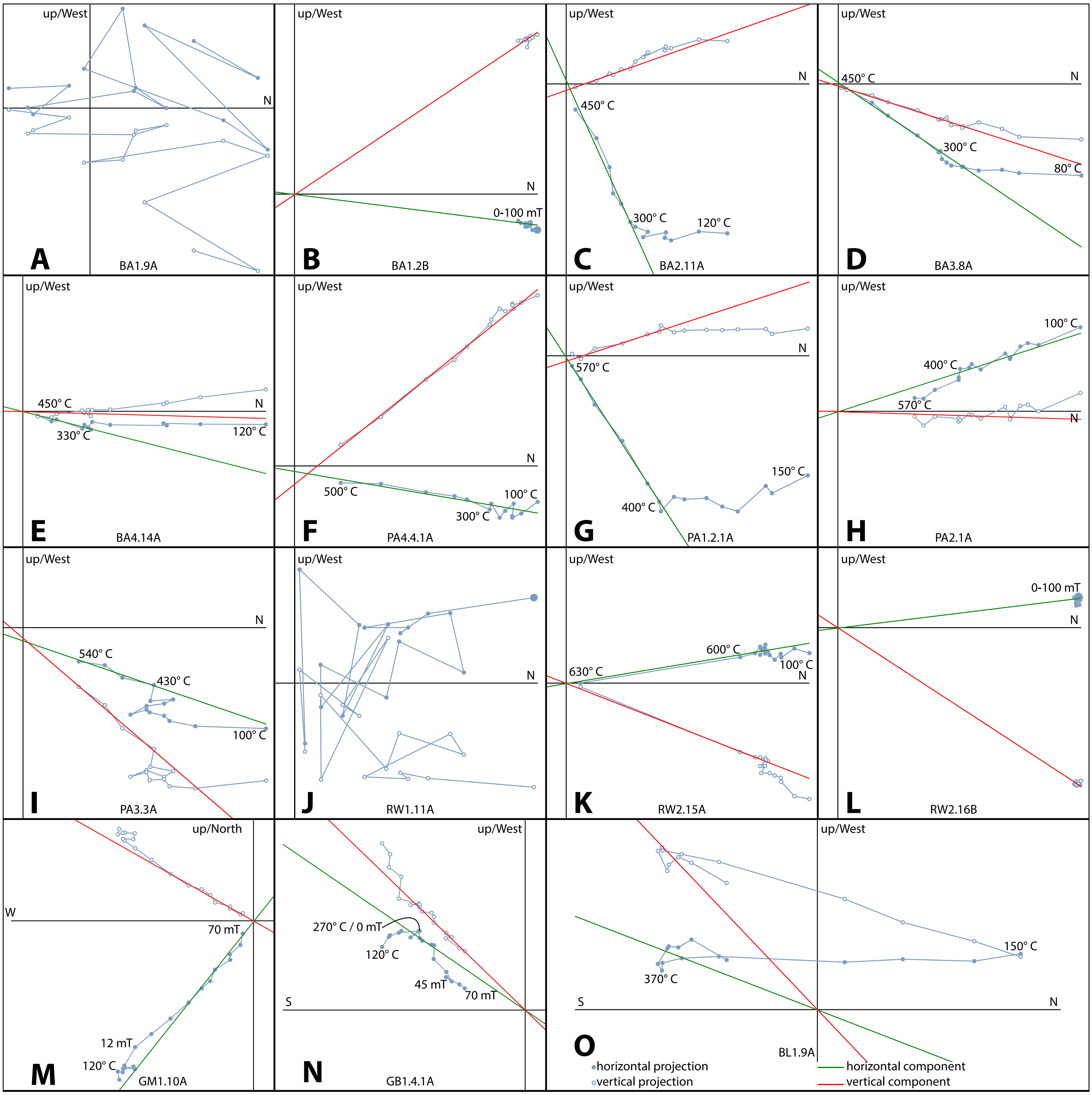

Fig. 4. Tilt-corrected Zijderveld diagrams of representative samples.

additional sources of scatter, while values of $A95 < A95_{min}$ represent low dispersion (high K-values, as with individual lava flows) and likely underrepresent PSV. All methods used are available on Paleomagnetism.org. In the online supplementary information, we provide all the demagnetisation results and interpretations as *.*dir* files that are easily imported into Paleomagnetism.org. Similarly, all statistical results including custom made apparent polar wander paths (APWPs) are provided as an *.*pmag* file.

3.2. Biostratigraphy

Benthic and planktonic foraminifera and algae of six samples from limestones of the Woyla Arc were dated based on BouDagher-Fadel (2015, 2008) relative to the biostratigraphic timescale of Gradstein et al. (2012). The faunal assemblage and the age range are reported in the Supplementary Material.

4. Results

Samples were collected at thirteen sites in sedimentary rocks and volcaniclastic rocks of the Woyla Arc, the oceanic accretionary assemblage and of the West Sumatra Block (Fig. 2) at the sparse locations where these rocks are exposed. Representative Zijderveld diagrams are shown in Fig. 4. The interpreted ChRM directions are shown in Fig. 5. The statistical properties of each site are shown in Table 1.

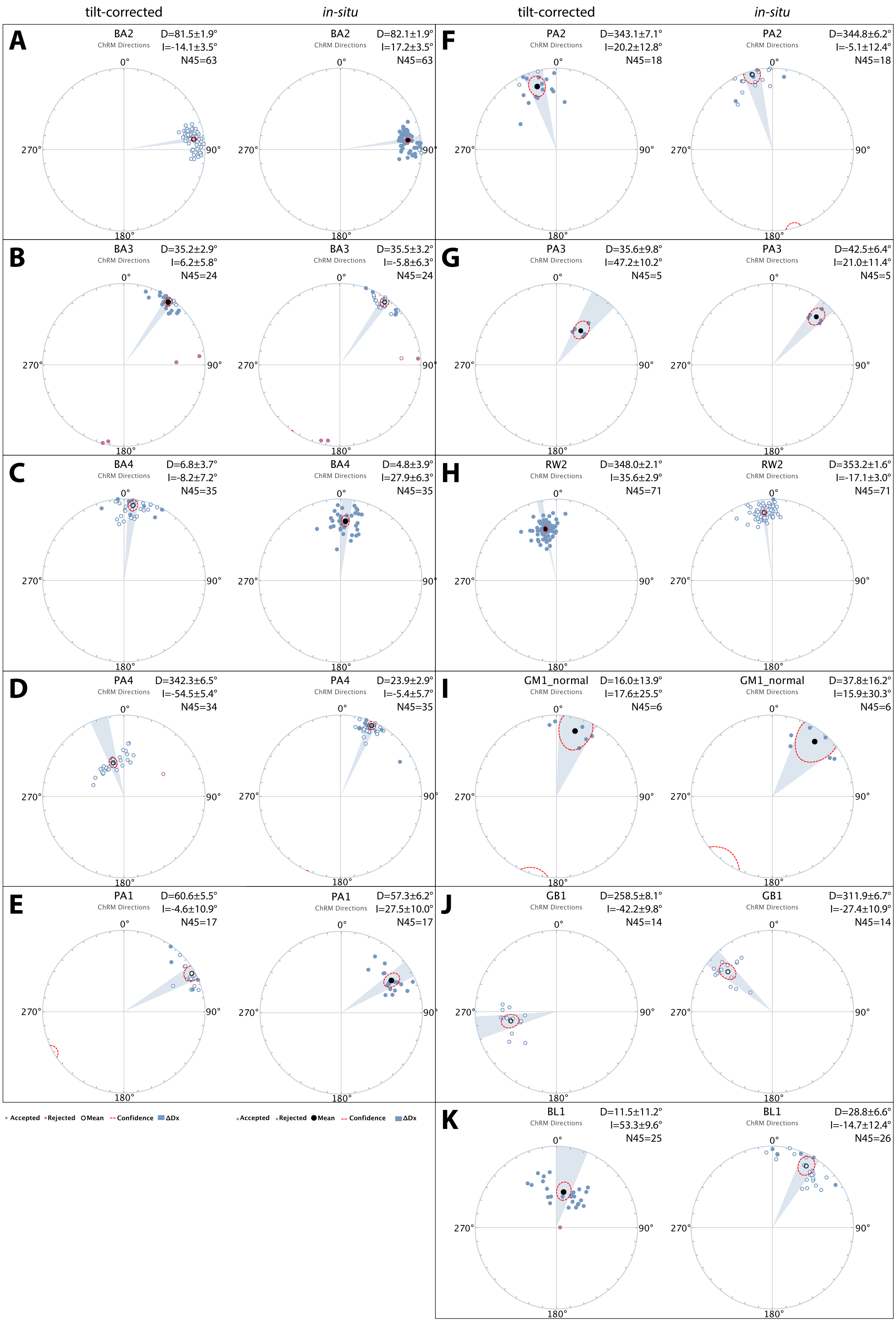

Fig. 5. Equal area projections of interpreted ChRM directions per site in tilt-corrected coordinates and *in-situ* coordinates.

Table 1

Statistical parameters of sampling sites. N: total number of interpreted ChRM directions; N_{45}: number of ChRM directions after 45° cut-off; $D \pm \Delta D_x$: declination and 95% confidence interval following Butler (1992); $I \pm \Delta I_x$; inclination and 95% confidence interval following Butler (1992); K: precision parameter of VGP distribution following Fisher (1953); $A95$: 95% cone of confidence on VGP distribution; $A95_{min}$ and $A95_{max}$: N-dependent confidence envelope for $A95$ values following Deenen et al. (2011); λ, λ_{min} and λ_{max}: paleolatitude, and minimum and maximum paleolatitude.

Site	Assemblage	Age range		GPS position		Bedding	N	Tectonic coordinates												Geographic coordinates											
		Stratigraphic	Numerical	Latitude	Longitude			N_{45}	D	ΔD_x	I	ΔI_x	K	$A95$	$A95_{min}$	$A95_{max}$	λ	λ_{min}	λ_{max}	N_{45}	D	ΔD_x	I	ΔI_x	K	$A95$	$A95_{min}$	$A95_{max}$	λ	λ_{min}	λ_{max}
BA1	Woyla Arc	Late Jurassic–Early Cretaceous	163.5–100.5 Ma	5.510520	95.278390	130/70	–	–	–	–	–	–	–	–	–	–	–	–	–	–	–	–	–	–	–	–	–	–	–	–	–
BA2	Woyla Arc	Late Jurassic–Early Cretaceous	163.5–100.5 Ma	5.373784	95.256141	310/40	63	63	81.5	1.9	−14.1	3.5	95.6	1.8	2.3	6.0	−7.1	−9.0	−5.3	63	82.1	1.9	17.2	3.5	91.9	1.9	2.3	6.0	8.8	7.0	10.7
BA3	Woyla Arc	Aptian	126.3–113.0 Ma	5.172197	95.307377	185/30	24	28	35.2	2.9	6.2	5.8	102.2	2.9	3.4	11.1	3.1	0.2	6.1	28	35.5	3.2	−5.8	6.3	88.9	3.2	3.4	11.1	−2.9	−6.1	0.2
BA4	Woyla Arc	Albian	113.0–100.5 Ma	5.094386	95.366598	290/40	35	35	6.8	3.7	−8.2	7.2	45.1	3.6	2.9	8.7	−4.1	−7.8	−0.5	35	4.8	3.9	27.9	6.3	41.8	3.8	2.9	8.7	14.8	11.2	18.8
PA4	Woyla Arc	Early Aptian–Early Albian	126.3–105 Ma	−1.073028	100.440750	350/30	34	35	342.3	6.5	−54.4	5.4	22.1	5.4	2.9	8.9	−34.9	−40.6	−29.9	35	23.9	2.9	−5.4	5.7	72.0	2.9	2.9	8.7	−2.7	−5.6	0.2
PA1	Ngalau Ocean	Aalenian–Early Bajocian	174.1–168.3 Ma	−0.955858	100.489290	100/30	17	17	60.6	5.5	−4.6	10.9	43.6	5.5	3.9	13.8	−2.3	−7.9	3.2	17	57.3	6.2	27.5	10.0	36.9	6.0	3.9	13.8	14.6	9.0	21.0
PA2	W. Sumatra	Late Jurassic–Early Cretaceous	163.5–100.5 Ma	−1.095900	100.475000	150/28	18	18	343.1	7.1	20.2	12.8	25.3	7.0	3.8	13.3	10.4	3.7	18.0	18	344.8	6.2	−5.1	12.4	31.8	6.2	3.8	13.3	−2.6	−9.0	3.6
PA3	W. Sumatra	Late Jurassic–Early Cretaceous	163.5–100.5 Ma	−1.073028	100.440750	328/68	5	5	35.6	9.8	47.2	10.2	80.4	8.6	6.3	29.7	28.4	20.7	38.1	5	42.5	6.4	21.0	11.4	148.7	6.3	6.3	29.7	10.9	4.8	17.6
RW1	W. Sumatra	Late Jurassic	163.5–145.0 Ma	−2.117255	102.008910	100/48	–	–	–	–	–	–	–	–	–	–	–	–	–	–	–	–	–	–	–	–	–	–	–	–	–
RW2	W. Sumatra	Late Jurassic	163.5–145.0 Ma	−2.115869	101.979570	110/60	71	71	348.0	2.1	35.6	2.9	73.7	2.0	2.2	5.6	19.7	17.8	21.7	71	353.2	1.6	−17.1	3.0	112.5	1.6	2.2	5.6	−8.8	−10.4	−7.2
GM1	Woyla Arc	116 ± 3 Ma	119–113 Ma	−3.803093	103.176780	205/65	6	6	16.0	13.9	17.6	25.5	24.9	13.7	5.9	26.5	9.0	−4.0	25.1	6	37.8	16.2	15.9	30.3	18.4	16.0	5.9	26.5	8.1	−7.3	27.6
GB1	Ngalau Ocean	>117 Ma	>117 Ma	−4.477090	104.167800	275/22	14	14	258.5	8.1	−42.2	9.8	30.0	7.4	4.2	15.6	−24.4	−32.6	−17.7	14	311.9	6.7	−27.4	10.9	38.6	6.5	4.2	15.6	−14.5	−21.5	−8.4
BL1	W. Sumatra	Aptian–Albian	126.3–100.5 Ma	−5.554367	105.185150	140/78	25	26	11.5	11.2	53.3	9.6	10.8	9.3	3.3	10.8	33.8	25.5	44.3	26	28.8	6.6	−14.7	12.4	20.0	6.5	3.3	10.5	−7.5	−14.4	−1.2

4.1. Northern Sumatra

We sampled limestones associated with the arc assemblage of the Woyla Group at four sites along the road from Banda Aceh to Lamno (Fig. 2b). Sites BA1 and BA2 correspond to the Raba Limestone Formation (Bennett et al., 1981) and sites BA3 and BA4 to the Lamno Limestone Formation (Bennett et al., 1981). The Lamno Limestone Formation yielded faunal assemblages with a Late Jurassic to Early Cretaceous age range and the Raba Limestone is correlated to have a similar age range (Bennett et al., 1981).

4.1.1. Raba limestone formation

At site BA1, we sampled a ∼14 m thick interval of dark-grey, thin-bedded (∼10 cm) limestones exposed in an active quarry. Thin section analysis revealed that the limestone is completely recrystallized. Twenty-one samples were demagnetised with AF demagnetisation and 16 with thermal demagnetisation. Intensities after the first heating step of 80 °C are below 70 μA/m and samples have a poor magnetic signal, characterised by chaotic demagnetisation behaviour (Fig. 4a). Some AF data show higher intensities (∼1000 μA/m) but the component does not decay towards the origin at the highest AF field (100 mT) (Fig. 4b), indicating the presence of a high-coercive mineral. Because of the lack of interpretable directions, we discard this site.

At site BA2 we sampled a ∼12 m thick interval of dark-grey thin-bedded limestone. Thin section analysis revealed that the limestone is completely recrystallized. Thirty-nine samples were demagnetised by AF and 25 samples thermally. The intensity of the samples is low (∼1000–2000 μA/m) with some stronger samples ranging to 8000 μA/m. At low temperatures/alternating fields, Zijderveld diagrams reveal a direction coinciding with the recent field, i.e. the geocentric axial dipole (GAD) field at the present latitude. At higher temperatures and fields there is a linear decay toward the origin from 300 °C/35 mT, with full demagnetisation at 480 °C suggesting titanomagnetite as dominant carrier (Fig. 4c). One sample yielded no interpretable direction. The tilt-corrected ChRM is $D = 81.5 \pm 1.9°$, $I = -14.1 \pm 3.5°$ and the *in-situ* ChRM is $D = 82.7 \pm 1.9°$, $I = 17.2 \pm 3.5°$ (Fig. 5a, Table 1). The *in-situ* $A95$ (1.9°) is smaller than $A95_{min}$ (2.3°), indicating that PSV may have been insufficiently sampled, or is partly averaged within samples.

4.1.2. Lamno limestone formation

At site BA3 we sampled a 50 m thick interval of dark-grey, thick-bedded limestones. We refined a previously assigned Late Jurassic to Early Cretaceous age range (Bennett et al., 1981) to the Aptian (126.3–113.0 Ma) (Supplementary Material). Fifteen samples were measured with AF demagnetisation and 13 by thermal demagnetisation. Initial intensities are relatively low (∼1000 μ/m). Zijderveld diagrams reveal a direction coinciding with the recent field at low temperatures/intensities. The linear decay towards the origin from 300 °C with full demagnetisation at 450 °C (Fig. 4d), suggests that the magnetisation is carried by titanomagnetite. Two directions are of reversed polarity, antipodal to the normal cluster, possibly recording the early Aptian M0r event (Gradstein et al., 2012). Four directions were rejected after 45° cut-off (Fig. 5b). The tilt-corrected ChRM is $D = 35.2 \pm 2.9°$, $I = 6.2 \pm 5.8°$ and the *in-situ* ChRM is $D = 35.5 \pm 3.2°$, $I = -5.8 \pm 6.3°$ (Table 1), with the tilt-corrected $A95$ (2.9°) being smaller than $A95_{min}$ (3.4°), suggesting PSV may have been partly averaged within samples.

At site BA4 we sampled a ∼70 m thick interval of thick-bedded limestones exposed along a road east of Lamno leading towards the mountains inland. Thin section analysis revealed that the limestone is partly recrystallized. We refined a previously assigned Late Jurassic to Early Cretaceous age range (Bennett et al., 1981) to the Albian (113.0–100.5 Ma) (Supplementary Material). Twenty samples were measured by AF demagnetisation and 15 by thermal demagnetisation. Zijderveld diagrams show a linear decay to the origin from 330 °C, with full demagnetisation at 450 °C, suggesting titanomagnetite as dominant carrier (Fig. 4e). No samples were rejected after 45° cut-off (Fig. 5c). The tilt-corrected ChRM is $D = 6.8 \pm 3.7°$, $I = -8.2 \pm 7.2°$ and the *in-situ* ChRM is $D = 4.8 \pm 3.9°$, $I = 27.9 \pm 6.3°$ (Table 1), with $A95$ between $A95_{min}$ and $A95_{max}$.

4.2. Central Sumatra

Rock units in Middle Sumatra correlated to the Woyla Group are exposed near Padang and in the Rawas Mountains (Fig. 2a, c). The Woyla Arc assemblage was sampled at site PA4 in the Lubuk Peraku Limestone (McCarthy et al., 2001) that is overlain by the Golok Tuff (McCarthy et al., 2001). The oceanic assemblage was sampled at site PA1 in the Ngalau Chert, which occurs as imbricated thrust slices between limestones (McCarthy et al., 2001). Sedimentary rocks of the West Sumatra continental margin were sampled at four sites (PA2 and PA3 in the Siguntur Formation (Rosidi et al., 1976) and sites RW1 and RW2 in the Penata Formation (Suwarna et al., 1994)).

4.2.1. Lubuk Peraku limestone

At site PA4 we collected five hand samples from a 3 m thick interval of massive bedded limestones exposed along the Lubuk Peraku River at the village of Indarung (Fig. 2c). We refined a previously assigned Late Jurassic to Early Cretaceous age range (Yancey and Alif, 1977) to early Aptian–early Albian (Supplementary Material). From these samples, we derived core samples in the lab, of which 28 samples were thermally demagnetised and 7 with AF. Initial intensities of most samples are ∼1500 μA/m, with a few up to 5000 μA/m. The Zijderveld diagrams reveal a component with a linear decay to the origin from 350 °C, with full demagnetisation at 500 °C suggesting titanomagnetite as dominant carrier (Fig. 4f). One sample was rejected after 45° cut-off (Fig. 5d). The tilt-corrected ChRM is $D = 342.3 \pm 6.5°$, $I = -54.4 \pm 5.4°$ and the *in-situ* ChRM is $D = 23.9 \pm 2.9°$, $I = -5.4 \pm 5.7°$ (Table 1). We observe that the *in-situ* $A95$ is equal to $A95_{min}$ (2.9°) indicating that PSV was insufficiently sampled.

4.2.2. Ngalau Chert

At the abandoned Ngalau Quarry in Indarung (Site PA1; Fig. 2c), we collected five oriented hand samples from a 10 m thick interval of Middle Jurassic (Aalenian–lower Bajocian; McCarthy et al., 2001) bedded radiolarian chert belonging to the oceanic assemblage. From these samples, we derived core samples in the lab, of which we derived directions from 12 thermally and 5 AF demagnetised samples. Initial intensities are very low (<300 μA/m). Most samples show a clear component coinciding with the recent field, followed by a linear decay to the origin from 400 °C up to temperatures of 570 °C, suggesting magnetite as the dominant carrier (Fig. 4g). The tilt-corrected ChRM is $D = 60.6 \pm 5.5°$, $I = -4.6 \pm 10.9°$ and the *in-situ* ChRM is $D = 57.3 \pm 6.2°$, $I = 27.5 \pm 10.0°$ (Fig. 5e, Table 1), with $A95$ between $A95_{min}$ and $A95_{max}$.

4.2.3. West Sumatra continental margin

At site PA2, exposed at a waterfall near the road from Padang to Siguntur (Fig. 2c), we sampled a 4 m thick interval of shales of the Siguntur Formation. Rosidi et al. (1976) reported an age range of Late Jurassic–Early Cretaceous, which we were unable to refine further. We demagnetised 9 samples thermally, and 9 by AF. Initial intensities are typically below 500 μA/m. Zijderveld diagrams show noisy demagnetisation behaviour, but overall decay towards the origin with full demagnetisation at 470–570 °C, suggesting magnetite as dominant carrier (Fig. 4h). One sample yielded no interpretable direction. No directions were rejected after 45° cut-off (Fig. 5f). The tilt-corrected ChRM is $D = 343.1 \pm 7.1°$, $I = 20.2 \pm 12.8°$ and the *in-situ* ChRM is $D = 344.8 \pm 6.2°$, $I = -5.1 \pm 12.4°$ (Table 1), with $A95$ between $A95_{min}$ and $A95_{max}$.

At site PA3, three cores yielded six samples that were collected from a 2 m thick interval of quarzitic sandstones of the Siguntur Formation, exposed along the road from Padang to Siguntur (Fig. 2c). Three samples were demagnetised by AF and the other three thermally. Initial intensities are ∼1000–1500 μA/m. Thermal demagnetisation diagrams reveal three components, of which the low-temperature component resembles the recent field (Fig. 4i). The high temperature component decays linearly to the origin between 430 °C and 540 °C, suggesting (titano)magnetite as the dominant carrier. All samples are of normal polarity. One sample yielded no interpretable direction. No directions were rejected after 45° cut-off (Fig. 5g). The tilt-corrected ChRM is $D = 35.6 \pm 9.8°$, $I = 47.2 \pm 10.2°$ and the *in-situ* ChRM is $D = 42.5 \pm 6.4°$, $I = 21.0 \pm 11.4°$ (Table 1). The *in-situ* $A95$ is equal to $A95_{\mathrm{min}}$ (6.3°), suggesting that PSV was insufficiently sampled. This is in line with the high K value, which is typical for spot readings of the field. We therefore discard this site from further analysis.

Along the road from Bangko to Lake Kerinci, we sampled sites RW1 and RW2 in exposures of the Peneta Formation that was previously dated at Middle Jurassic–Early Cretaceous (Suwarna et al., 1994), whereas Beauvais et al. (1988) reported a Late Jurassic age for the limestone members of the formation.

At site RW1, we sampled a ∼2 m thick interval of calcareous sandstones and siltstones of the Mersip Limestone Member. Twelve samples were demagnetised thermally and five by AF. The intensity is very low (∼100 μA/m) and demagnetisation diagrams are chaotic (Fig. 4j). No ChRM directions were interpreted and site RW1 was discarded from further analysis.

At site RW2 we sampled a 50 m thick interval of red tuffaceous shales. A total of 43 samples were demagnetised thermally and 29 with AF. Initial intensities are high (∼20000 μA/m). demagnetisation behaviour varies strongly between AF and thermally demagnetised samples. AF demagnetisation diagrams reveal a tight cluster at high intensities, without complete demagnetisation (Fig. 4l), pointing to a high coercivity mineral. Thermal demagnetisation led to gradual decay towards the origin at temperatures well above 600 °C (Fig. 4k). We thus interpret the dominant magnetic carrier as hematite. The direction indicated by the AF cluster yields a similar direction as the component demagnetizing towards the origin using thermal demagnetisation and both were used to interpret the ChRM direction. One sample yielded an anomalous direction and was therefore discarded. The tilt-corrected ChRM is $D = 348.0 \pm 2.1°$, $I = 35.6 \pm 2.9°$ and the *in-situ* ChRM is $D = 353.2 \pm 1.6°$, $I = -17.1 \pm 3.0°$ (Fig. 5h, Table 1). The *in-situ* $A95$ (1.6°) is smaller than $A95_{min}$ (2.2°).

4.3. Southern Sumatra

We sampled volcaniclastic sedimentary rocks of the Saling Formation (Gafoer et al., 1992) belonging to the Woyla Arc assemblage in the Gumai Mountains (site GM1), cherts belonging to the oceanic assemblage exposed in the Garba Mountains (site GB1) and turbiditic sandstones exposed near the city of Bandar Lampung belonging to the West Sumatra Block continental arc assemblage (site BL1) (Fig. 2a).

4.3.1. Saling Formation

At site GM1, we collected eight samples from a ∼4 m wide exposure of volcaniclastic sedimentary rocks of the Saling Formation (Gafoer et al., 1992) along the Serampo River in the Gumai Mountains. The Saling Formation is intruded by a diorite dyke with a K–Ar age of 116 ± 3 Ma (Aptian), interpreted to be coeval with the volcaniclastic sediments (Gafoer et al., 1992). Samples were thermally demagnetised to 270 °C and further demagnetised by AF. Initial intensities are <500 μA/m. The Zijderveld diagrams reveal a linear decay to the origin (Fig. 4m). Six samples are of reversed polarity, possibly recording the early Aptian M0r event (Gradstein et al., 2012). After inverting these reversed directions to normal polarity, the tilt-corrected ChRM is $D = 16.0 \pm 13.9°$, $I = 17.6 \pm 25.5°$ and the *in-situ* ChRM is $D = 37.8 \pm 16.2°$, $I = 15.9 \pm 30.3°$ (Fig. 5i, Table 1), with $A95$ between $A95_{min}$ and $A95_{max}$.

4.3.2. Garba Formation

At site GB1 we collected five hand samples from a 2 m thick interval of bituminous shales of the Situlanglang chert member of the Garba Formation (Gafoer et al., 1994) exposed along a tributary of the Kumering River near the Garba Mountains (Fig. 2a). The chert member did not yield age-diagnostic fossils (Barber, 2000). A minimum age for the Garba Formation comes from the cross-cutting composite Garba Pluton, which yielded K–Ar ages of 117–79 Ma (Gafoer et al., 1994; McCourt et al., 1996). From the hand samples, 15 core samples were derived in the laboratory. Due to the high organic matter contents, samples were only demagnetised thermally to 270 °C, and subsequently demagnetised by AF. Initial intensities were ∼300 μA/m. Most demagnetisation diagrams revealed two components, whereby the higher coercivity component decays approximately towards the origin (Fig. 4n). Samples that were not subjected to thermal demagnetisation reveal a high coercive component that is not removed by alternating field demagnetisation. This component is likely carried by goethite. One samples yielded an anomalous direction. The tilt-corrected ChRM is $D = 258.5 \pm 8.1°$, $I = -42.2 \pm 9.8°$ and the *in-situ* ChRM is $D = 311.9 \pm 6.7°$, $I = -27.4 \pm 10.9°$ (Fig. 5j, Table 1), with $A95$ between $A95_{min}$ and $A95_{max}$.

4.3.3. Menanga Formation

At site BL1, along the Menanga River near Bandar Lampung, we sampled a 4 m wide exposure of a sequence of thin turbiditic sandstones and siltstones of the Menanga Formation (Andi Mangga et al., 1994). Previous studies dated the limestones interbedded in the Menanga formation as Aptian–Albian (Andi Mangga et al., 1994; Zwierzycki, 1932), which we adopt as age range for the turbiditic sequence. Eighteen samples were demagnetised thermally, and 10 by AF. Intensities of the samples are high, ranging from 1.5 to 200 mA/m. Zijderveld diagrams reveal two types of demagnetisation behaviour. One group of samples show linear demagnetisation towards the origin up to temperatures of 570 °C. The second group of samples shows three components, with linear decay to the origin from 370–570 °C (Fig. 4o), suggesting magnetite as dominant magnetic carrier. Two samples yielded no interpretable directions. Three samples yielded reversed directions antipodal to the normal cluster. After converting these directions to normal polarity, no samples were rejected after 45° cut-off for *in-situ* directions, but one sample was rejected after 45° cut-off and tilt-correction (Fig. 4k). The tilt-corrected ChRM is $D = 11.5 \pm 11.2°$, $I = 53.3 \pm 9.6°$ and the *in-situ* ChRM is $D = 28.8 \pm 6.6°$, $I = -14.7 \pm 12.4°$ (Table 1), with $A95$ between $A95_{min}$ and $A95_{max}$.

5. Discussion

5.1. Paleolatitude reconstruction of the Woyla Arc and West Sumatra Block

Plate tectonic reconstructions suggest that the West Sumatra Block accreted to Sundaland in the Late Triassic–Early Jurassic (Barber et al., 2005; Barber and Crow, 2009; Metcalfe, 2013). We therefore compare our paleomagnetic results from the West Sumatra Block with the global APWP (GAPWaP) of Torsvik et al. (2012) rotated into the coordinates of Sundaland. To this end, we use the tool on paleomagnetism.org described in Li et al. (2017) that allows calculating the global GAPWaP into the coordinates of a restored block when Euler poles of that block relative to South Africa are provided. We use the estimated Euler poles of Sundaland of Advokaat et al. (under review) (Fig. 7a), which show no relative rotation to Eurasia and the Atlantic plate circuit of Torsvik et al. (2012) and Seton et al. (2012). The tilt-corrected inclination of site PA2 indeed coincides with the APWP of Sundaland during the Late Jurassic (Figs. 5f, 6a), but also the *in-situ* inclination overlaps with the APWP of Sundaland in the Late Jurassic–Early Cretaceous. As we do not have independent confirmation of the primary nature of the magnetisation of this site, it is also possible that this site was remagnetised during the mid-Cretaceous collision of the Woyla Arc with the West Sumatra margin. The tilt-corrected inclinations of sites PA3, RW2 and BL1 are higher than predicted by the APWP. However, we have no independent confirmation of the primary nature of the magnetisation of these sites. Because the *in-situ* inclination of PA3 and BL1 overlaps with the Sundaland APWP, we suspect that these sites may have been remagnetised. The *in-situ* inclination of site RW2 is below the Sundaland APWP, but given that its magnetisation is carried by hematite, which may form in laterite as alteration product of magnetite, we suspect this site may have been remagnetised and was subsequently further tilted during later deformation.

Four out of six sites from the Woyla Arc assemblage (BA2, BA3, BA4, GM1) provide tilt-corrected inclinations that suggest near-equatorial latitudes (Figs. 5a–c, 5i). Because sites BA2 and BA4 are recrystallized and their *in-situ* inclination coincides with the Sundaland APWP, we suspect these sites were remagnetised during the mid-Cretaceous collision of the Woyla Arc with the West Sumatra margin. Site PA4 has a high tilt-corrected inclination, but because the *in-situ* inclination coincides with the Sundaland APWP, we suspect that also this site was remagnetised during the mid-Cretaceous collision of the Woyla Arc with the West Sumatran margin.

Finally, we examine sites PA1 and GB1 obtained from oceanic assemblage rocks exposed between the Woyla Arc and the West Sumatra Block. These rocks were thus likely derived from the once intervening ocean basin that was consumed by subduction below the Woyla Arc and the West Sumatra Block (Fig. 3). Here, we call this conceptual ocean the Ngalau Ocean, after the Ngalau Chert. No fold test was possible for sites PA1 and GB1 and we have thus no independent confirmation of primary magnetisation. The tilt-corrected inclination ($-4.6 \pm 10.9°$) of site PA1 indicates a near-equatorial paleolatitude, but has a high *in-situ* inclination of $27.5 \pm 10.0°$ that would suggest a paleolatitude of $\lambda = 14.6°$N or S ($\lambda_{min} = 9.0°$, $\lambda_{max} = 21.0°$). Tilting likely occurred upon or after accretion of the cherts of this site to the Woyla Arc, or to the West Sumatra Block. Neither of these has been at a latitude of 14.6°N or S since the Cretaceous, and it is thus unlikely that the magnetisation post-dates the tilting. Conversely, site GB1 has a high tilt-corrected inclination ($-42.2 \pm 9.8°$) which would suggest a paleolatitude of $\lambda = 28.4°$N or S ($\lambda_{min} = 20.7°$, $\lambda_{max} = 38.1°$). If the magnetisation is primary, this would suggest a ∼3000 km paleolatitudinal plate motion within the Ngalau ocean basin between sites PA1 and GB1 since the Late Jurassic. We consider this unlikely. On the other hand, the *in-situ* inclination of site GB1 is $-21.0 \pm 11.4°$. If the magnetisation postdates tilting it should then have been acquired at a paleolatitude of 10.9°N or S ($\lambda_{min} = 4.8°$, $\lambda_{max} = 17.6°$), which is within range of both the Woyla Arc and the West Sumatra Block during collision in the mid-Cretaceous. We thus tentatively interpret the data to suggest that the rocks derived from the Ngalau Ocean were also at equatorial latitudes, with site PA1 carrying a primary magnetisation, and site GB1 carrying a post-tilt magnetisation.

In summary, our sites that likely carry a primary magnetisation suggest that the Woyla Arc remained at a near-equatorial latitudes in the Early Cretaceous. All other sites, including those from the conceptual Ngalau Ocean, either carry magnetisations that in tectonic coordinates also show equatorial latitudes, or that have equatorial inclinations in *in-situ* coordinates, which may be explained by syn-collisional remagnetisation. Throughout the Cretaceous, the West Sumatra Block, to which the Woyla Arc accreted in the mid-Cretaceous, was also at equatorial latitudes, suggesting that the Woyla Arc did not undergo significant N–S directed motions during its approach to Sundaland.

5.2. Plate kinematic reconstruction: introducing the Ngalau Plate

The structure and composition of Sumatra led Barber et al. (2005) to suggest that the Woyla Arc formed on oceanic lithosphere that was separated from Eurasia by two subduction zones that consumed oceanic lithosphere (what we here call the Ngalau Ocean), which subducted westward below the Woyla Arc and eastward below Sundaland. We now test whether the lithosphere on which the Woyla Arc was situated may have been part of one of the major surrounding plates, or if not, whether yet another plate needs to be invoked to explain the paleolatitudes of the Woyla Arc.

First, Hall (2012) and Metcalfe (2013) suggested that the Woyla Arc may have formed on lithosphere of the Indian plate, to account for the low paleolatitude of Woyla rocks reported by Haile (1979). Second, van Hinsbergen et al. (2012) and Huang et al. (2015a) argued that a plate that carried a Tibetan Himalayan microcontinent broke off India and underwent a northward flight relative to the main Indian continent between Early and latest Cretaceous time. This model aims to account for low, near-northern Indian paleolatitudes derived from Lower Cretaceous, Triassic, and Ordovician rocks of the Tibetan Himalaya suggesting a separation of <800 km (consistent with West-Australian margin reconstructions of Gibbons et al. (2012), but a >2000 km wide separation at the time of early Eocene collision as required by paleomagnetic data of southern Tibet. If the Woyla Arc formed on the Indian plate in the Early Cretaceous, it would have undergone this northward flight. We test this scenario using the recent Euler poles for the Tibetan Himalaya relative to India of van Hinsbergen et al. (2018, 2011) and Li et al. (2017). Third, we test whether the Woyla Arc may have formed on the Australian plate as suggested by Metcalfe (1996). We constructed these scenarios using the online platform paleomagnetism.org (Koymans et al., 2016), whereby we plot our data against the GAPWaP (Torsvik et al., 2012) in coordinates of India, the conceptual Tibetan Himalaya plate, or Australia. Only tilt-corrected inclinations of the sites with inferred primary magnetisations are plotted. In all scenarios we assume a ∼95 Ma age of Woyla–Sundaland collision, corresponding to the youngest K–Ar age from metamorphic rocks from the West Sumatra margin (Koning, 1985).

If the Woyla Arc was formed on the edge of the conceptual Tibetan Himalayan plate, it would have undergone a ∼40° northward latitudinal motion between ∼130 and 95 Ma (Fig. 7b). The predicted APWP is clearly inconsistent with our data from the Woyla Arc (Fig. 6b). If no Tibetan Himalayan plate ever formed (e.g. Ingalls et al., 2016), which would require that all paleomagnetic data from the Tibetan Himalaya are unreliable and 1000s of km of Indian lithosphere subducted without leaving a trace (van Hinsbergen et al., 2012, 2018), the Woyla Arc may have formed on India. In this scenario, the Woyla Arc would have experienced a ∼25° northward latitudinal motion between 130 and 95 Ma (Fig. 7b), which predicts our data better, but is still inconsistent with site GM1 (Fig. 6b). Finally, if the Woyla Arc formed on the Australian plate it would have moved eastwards relative to Eurasia and Sundaland, over a distance of ∼1700 km, and remained at near-equatorial latitudes between 130 and 95 Ma (Fig. 7). The predicted APWP is consistent with our data (Fig. 6b). Hence, we propose that the Woyla Arc has likely formed on the Australian plate, and that there is no kinematic requirement to invoke a more complex scenario in which the Woyla Arc formed on a plate independent from Australia, India, and the Tibetan Himalaya.

If the Woyla Arc formed on the Australian plate, the India-Australia plate boundary would have been located to the west of the Woyla Arc, and we may explore how a three-plate system of Australia–Ngalau–Eurasia (Sundaland) may have logically evolved prior to, during, and after Woyla Arc–Sundaland collision. Prior to the formation of the Woyla Arc, ∼E–W convergence of the East Gondwana Plate – to which both Australia and India belonged – relative to Sundaland was accommodated by a NE-dipping subduction zone under the West Sumatra continental margin, as shown by a belt of Jurassic–Cretaceous arc plutons (McCourt et al., 1996). At some stage at or prior to ∼130–122 Ma, a ∼westward intra-oceanic subduction initiated below the Australian plate above which the Woyla Arc formed (Fig. 7a). It is unclear why this subduction zone formed, but it may relate to the ∼130 Ma breakup of East Gondwana into Antarctica, Australia, and India (e.g. Gibbons et al., 2012; Seton et al., 2012). Also the cause for localising the Woyla trench remains open for speculation, but Barber et al. (2005) suggested westward subduction below the Woyla Arc may have initiated along a north–south transform fault. Either way, if we reconstruct the location of the Woyla Arc as part of the Australian plate, assuming a ∼95 Ma collision at Sumatra, we restore a trench ∼1700 km west of the West-Sumatra block at 130 Ma. We assume that the Woyla trench ended in a triple junction somewhere along the western margin of the West Burma Block (Fig. 7a). Equivalents of the Woyla Arc may exist in Myanmar (Barber and Crow, 2009; Mitchell, 1993). We are not aware of accreted intra-oceanic arcs of Early Cretaceous age in the Indus-Yarlung suture zone, while there was northward subduction below Tibet since at least 130 Ma (e.g. Guilmette et al., 2009). The Australia–India (or Tibetan Himalaya) plate boundary that also formed around 130 Ma (e.g. Gibbons et al., 2012; Seton et al., 2012; Van Hinsbergen et al., 2012) was likely located not far to the west of the Woyla Arc, and Tibetan Himalaya–Asia convergence drove south Tibetan subduction. We thus restore a ∼N–S striking Woyla trench, at a small angle to the NW–SE striking western Sundaland margin.

We thus infer a small, triangular Ngalau plate, caught between a transform fault in the south, and the west-dipping Woyla and east-dipping West Sundaland trenches that merged in a trench-trench-trench triple junction in the north (Fig. 7a). This inferred triangular geometry assumes that West Sumatra has not experienced major vertical axis rotations since the Late Jurassic. Previously, large rotations of Sundaland were postulated based on both CW and CCW declinations in rocks from the Malay Peninsula, where Otofuji et al. (2017) interpreted that the Malay Peninsula underwent a regional ∼70° CW rotation together with Indochina. This is inconsistent with paleomagnetic results from the Malay Peninsula, which show both CW and CCW declinations (Haile et al., 1983; Richter et al., 1999), and Indochina, which only indicate a 15° CW rotation in Cenozoic time (Li et al., 2017) and the rotations on the Malay peninsula are likely governed by local deformation. Governed by E–W Australia–Sundaland convergence, the Ngalau plate became consumed by subduction and its only relicts are preserved in the accretionary complexes of the Woyla Arc and the West Sumatra margin (McCarthy et al., 2001). In the configuration of Fig. 7, this convergence would have led to diachronous Woyla–Sundaland collision, younging southward, and associated southward migration of the triple junction. Such a southward migration remains speculative in the absence of hard constraints on

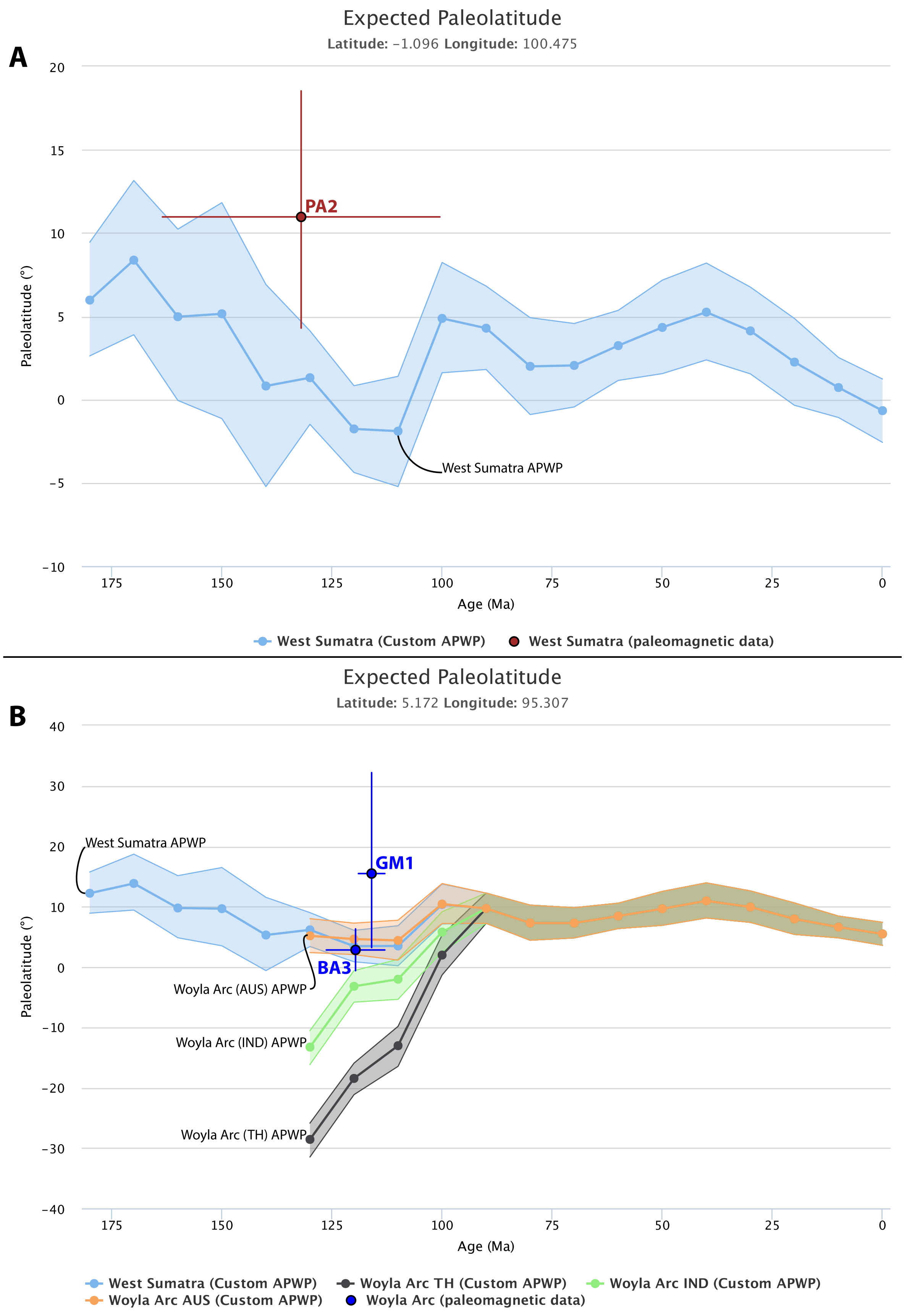

Fig. 6. A) Expected paleolatitude of West Sumatra (Sundaland) from Advokaat et al. (in press) and primary tilt-corrected paleomagnetic data from the West Sumatra continental margin (this study), B) Predicted paleolatitude for the Woyla Arc as part of the Tibetan Himalayan plate (grey), Indian plate (green), and Australian plate (orange) against primary tilt-corrected paleomagnetic data from the Woyla Arc (blue).

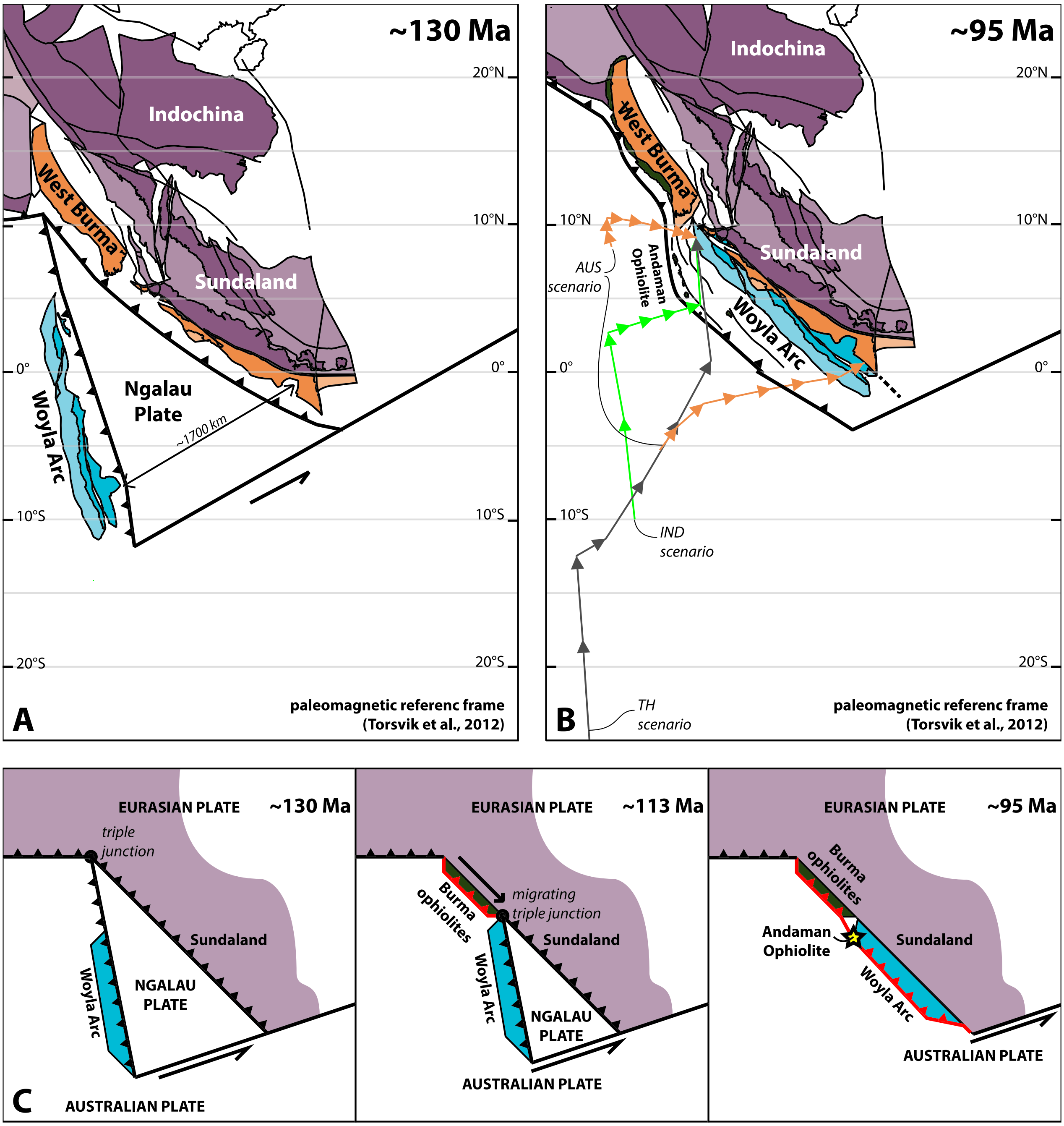

Fig. 7. A) Reconstruction at 130 Ma, the triangular Ngalau Plate is bordered to the west and east by two opposing subduction zones, and to the south by a transform fault, B) Reconstruction at 95 Ma: the triangular Ngalau Plate is entirely consumed by subduction. Motion paths between 130–95 Ma in 5 Ma time steps for scenarios where the Woyla Arc is part of Tibetan Himalayan plate (grey), Indian plate (green), and Australian plate (orange), C) Schematic kinematic scenario showing southward triple junction migration.

the age of collision. Following collision of the Woyla Arc with Sundaland, convergence between Sundaland and Australia continued (Seton et al., 2012), and must have been accommodated by renewed subduction (Barber et al., 2005). With the plate kinematic scenario as outlined in Fig. 7, the only stable triple junction arises if the post-collisional subduction zone is east-dipping, and necessarily locates west of the Woyla Arc so as to preserve its geological record. Possible records of this subduction polarity reversal following Woyla–Sundaland collision are found in supra-subduction ophiolites on the margin of West Burma (127–116 Ma, Liu et al., 2016; Singh et al., 2017) and the Andaman–Nicobar Islands (93.6 ± 1.6 Ma, Sarma et al., 2010).

6. Conclusions

In this study, we attempted to reconstruct the oceanic plate between the Woyla Arc and the western Sundaland margin. We show that the Woyla Arc formed above a west dipping subduction zone in the Early Cretaceous. Paleomagnetic data from limestones of the Woyla Arc indicate that these were formed and remained at equatorial latitudes. We tested plate kinematic scenarios where the Woyla Arc was part of the Tibetan Himalayan plate, the Indian plate and the Australian plate against paleomagnetic data. Scenarios where the Woyla Arc was part of the Tibetan Himalayan plate or Indian plate predict large latitudinal motions, inconsistent with our paleomagnetic data. Only a scenario where the Woyla Arc is part of the Australian Plate, which predicts ∼1700 km eastwards longitudinal motion relative to West Sumatra, is consistent with our paleomagnetic data.

We propose a reconstruction where the Ngalau Plate formed a triangular basin between the Woyla Arc and the western Sundaland margin, to account for the absence of accreted arc rocks in the Himalayas. As consequence of this triangular geometry, accretion of the Woyla Arc to the western Sundaland margin was diachronous, accommodated by a southward migrating triple junction. Continuing convergence of the Australia relative to Eurasia was accommodated by subduction polarity reversal behind the Woyla Arc, possibly recorded by Cretaceous ophiolites in the Indo-Burman Ranges and the Andaman-Nicobar Islands.

Acknowledgements

ELA and DJJvH acknowledge funding through ERC Starting Grant 306810 (SINK) to DJJvH. DJJvH acknowledges Netherlands Organization for Scientific Research (NWO) Vidi grant 864.11.004. ELA thanks Anthony Barber and Michael Crow for their introduction and discussion of the rocks of the Woyla Group. ELA and MLMB acknowledge the Indonesian government for research permits through RISTEK. ELA, MLMB and AR thank Edo Marshal, Adit Safriadi and Yudi Wandra for their help during sampling in Sumatra. MLMB thanks Dan Palcu for help during paleomagnetic analysis at Paleomagnetic Laboratorium 'Fort Hoofddijk'. We are greatly indebted to Pierrick Roperch for careful inspection of our data in a previous version of this manuscript, and thank Mathijs Koymans for help with data conversion. We thank Anthony Barber, John Geissman and an anonymous reviewer for their constructive comments.

Appendix A. Supplementary material

Supplementary material related to this article can be found online at https://doi.org/10.1016/j.epsl.2018.07.001.

References

Abrajevitch, A.V., Ali, J.R., Aitchison, J.C., Davis, A.M., Liu, J., Ziabrev, S.V., 2005. Neotethys and the India–Asia collision: insights from a palaeomagnetic study of the Dazhuqu ophiolite, southern Tibet. Earth Planet. Sci. Lett. 233, 87–102.
Advokaat, E.L., Marshall, N., Li, S., Spakman, W., Krijgsman, W., van Hinsbergen, D.J.J., in press. Cenozoic rotation history of Borneo and Sundaland, SE Asia, revealed by paleomagnetism, mantle tomography and kinematic reconstruction. Tectonics. https://doi.org/10.1029/2018TC005010.
Andi Mangga, S., Amiruddin Suwarti, T., Gafoer, S., Sidarto, 1994. Geology of the Kotaagung Quadrangle, Sumatra (1:250,000). Geol. Res. Dev. Centre, Bandung.
Barber, A.J., 2000. The origin of the Woyla Terranes in Sumatra and the Late Mesozoic evolution of the Sundaland margin. J. Asian Earth Sci. 18, 713–738.
Barber, A.J., Crow, M.J., 2009. Structure of Sumatra and its implications for the tectonic assembly of Southeast Asia and the destruction of Paleotethys. Isl. Arc 18, 3–20.
Barber, A.J., Crow, M.J., De Smet, M.E.M., 2005. Tectonic evolution. Mem. Geol. Soc. Lond. 31, 234–259.
Beauvais, L., Blanc, P., Bernet-Rollande, M.C., Maurin, A.F., 1988. Sedimentology of Upper Jurassic deposits in the Tembesi River area, central Sumatra. Bull. Geol. Soc. Malays. 22, 45–64.
Bennett, J.D., Bridge, Dm., Cameron, N.R., Djunuddin, A., Ghazali, S.A., Jeffery, D.H., Kartawa, W., Keats, W., Rock, N.M.S., Thomson, S.J., 1981. Geologic Map of the Banda Aceh Quadrangle, Sumatra. Geol. Res. Dev. Cent., Bandung, Indonesia.
BouDagher-Fadel, M.K., 2015. Biostratigraphic and Geological Significance of Planktonic Foraminifera. UCL Press.
BouDagher-Fadel, M.K., 2008. Evolution and Geological Significance of Larger Benthic Foraminifera. Elsevier.
Butler, R.F., 1992. Paleomagnetism: Magnetic Domains to Geologic Terranes. Blackwell Scientific Publications, Boston.
Cameron, N.R., Clarke, M.C.G., Aldiss, D.T., Aspden, J.A., Djunuddin, A., 1980. The geological evolution of northern Sumatra.
Deenen, M.H.L., Langereis, C.G., van Hinsbergen, D.J.J., Biggin, A.J., 2011. Geomagnetic secular variation and the statistics of palaeomagnetic directions. Geophys. J. Int. 186, 509–520.
Fisher, R., 1953. Dispersion on a sphere. Proc. R. Soc. Lond. Ser. A, Math. Phys. Eng. Sci. 217, 295–305.
Gafoer, S., Amin, T.C., Paedede, R., 1994. Geology of the Baturaja Quadrangle, Sumatra (1:250,000). Geol. Res. Dev. Centre, Bandung.
Gafoer, S., Amin, T.C., Pardede, R., 1992. Geology of the Bengkulu Quadrangle, Sumatra. Geol. Res. Dev. Centre, Indonesia.
Gibbons, A.D., Barckhausen, U., den Bogaard, P., Hoernle, K., Werner, R., Whittaker, J.M., Müller, R.D., 2012. Constraining the Jurassic extent of Greater India: tectonic evolution of the West Australian margin. Geochem. Geophys. Geosyst. 13.
Gradstein, F.M., Ogg, J.G., Schmitz, M., Ogg, G., 2012. The Geologic Time Scale 2012. Elsevier.
Guilmette, C., Hébert, R., Wang, C., Villeneuve, M., 2009. Geochemistry and geochronology of the metamorphic sole underlying the Xigaze ophiolite, Yarlung Zangbo Suture Zone, south Tibet. Lithos 112, 149–162.
Haile, N.S., 1979. Palaeomagnetic evidence for rotation and northward drift of Sumatra. J. Geol. Soc. Lond. 136, 541–546.
Haile, N.S., Beckinsale, R.D., Chakraborty, K.R., Hussein, A.H., Hardjono, T., 1983. Palaeomagnetism, geochronology and petrology of the dolerite dykes and basaltic lavas from Kuantan, West Malaysia. Bull. Geol. Soc. Malays. 16, 71–85. Ill, Map.
Hall, R., 2012. Late Jurassic? Cenozoic reconstructions of the Indonesian region and the Indian Ocean. Tectonophysics 570–571, 1–41. https://doi.org/10.1016/j.tecto.2012.04.021.
Huang, W., Hinsbergen, D.J.J., Lippert, P.C., Guo, Z., Dupont-Nivet, G., 2015a. Paleomagnetic tests of tectonic reconstructions of the India–Asia collision zone. Geophys. Res. Lett. 42, 2642–2649.
Huang, W., Van Hinsbergen, D.J.J., Maffione, M., Orme, D.A., Dupont-Nivet, G., Guilmette, C., Ding, L., Guo, Z., Kapp, P., 2015b. Lower Cretaceous Xigaze ophiolites formed in the Gangdese forearc: evidence from paleomagnetism, sediment provenance, and stratigraphy. Earth Planet. Sci. Lett. 415, 142–153.
Ingalls, M., Rowley, D.B., Currie, B., Colman, A.S., 2016. Large-scale subduction of continental crust implied by India–Asia mass-balance calculation. Nat. Geosci. 9, 848–853.
Johnson, C.L., Constable, C.G., Tauxe, L., Barendregt, R., Brown, L.L., Coe, R.S., Layer, P., Mejia, V., Opdyke, N.D., Singer, B.S., 2008. Recent investigations of the 0–5 Ma geomagnetic field recorded by lava flows. Geochem. Geophys. Geosyst. 9.
Kirschvink, J.L., 1980. The least-squares line and plane and the analysis of palaeomagnetic data. Geophys. J. Int. 62, 699–718.
Koning, T., 1985. Petroleum geology of the Ombilin intermontane basin, West Sumatra. In: Proc. Indonesian Petroleum Association 14th Annual Convention, pp. 117–137.
Koymans, M.R., Langereis, C.G., Pastor-Galán, D., van Hinsbergen, D.J.J., 2016. Paleomagnetism.org: an online multi-platform open source environment for paleomagnetic data analysis. Comput. Geosci. 127 (137), 93.
Li, S., Advokaat, E.L., van Hinsbergen, D.J.J., Koymans, M., Deng, C., Zhu, R., 2017. Paleomagnetic constraints on the Mesozoic–Cenozoic paleolatitudinal and rotational history of Indochina and South China: review and updated kinematic reconstruction. Earth-Sci. Rev. 171. https://doi.org/10.1016/j.earscirev.2017.05.007.
Liu, C.-Z., Chung, S.-L., Wu, F.-Y., Zhang, C., Xu, Y., Wang, J.-G., Chen, Y., Guo, S., 2016. Tethyan suturing in Southeast Asia: zircon U–Pb and Hf–O isotopic constraints from Myanmar ophiolites. Geology 44, 311–314.
McCarthy, A.J., Jasin, B., Haile, N.S., 2001. Middle Jurassic radiolarian chert, Indarung, Padang District, and its implications for the tectonic evolution of western Sumatra, Indonesia. J. Asian Earth Sci. 19, 31–44.
McCourt, W.J., Crow, M.J., Cobbing, E.J., Amin, T.C., 1996. Mesozoic and Cenozoic plutonic evolution of SE Asia: evidence from Sumatra, Indonesia. Geol. Soc. (Lond.) Spec. Publ. 106, 321–335.
Metcalfe, I., 2013. Gondwana dispersion and Asian accretion: tectonic and palaeogeographic evolution of eastern Tethys. J. Asian Earth Sci. 66, 1–33. https://doi.org/10.1016/j.jseaes.2012.12.020.
Metcalfe, I., 1996. Pre-Cretaceous evolution of SE Asian terranes. Geol. Soc. (Lond.) Spec. Publ. 106, 97–122.
Mitchell, A.H.G., 1993. Cretaceous–Cenozoic tectonic events in the western Myanmar (Burma)–Assam region. J. Geol. Soc. Lond. 150, 1089–1102.
Otofuji, Y., Moriyama, Y.T., Arita, M.P., Miyazaki, M., Tsumura, K., Yoshimura, Y., Shuib, M.K., Sone, M., Miki, M., Uno, K., 2017. Tectonic evolution of the Malay Peninsula inferred from Jurassic to Cretaceous paleomagnetic results. J. Asian Earth Sci. 134, 130–149.
Richter, B., Schmidtke, E., Fuller, M., Harbury, N., Samsudin, A.R., 1999. Paleomagnetism of Peninsular Malaysia. J. Asian Earth Sci. 17, 477–519.
Rosidi, H.M.D., Tjoksapoetro, S., Pendowo, B., 1976. The Geology of the Painan and Northeastern Part of the Muarasiberut Quadrangles, Sumatra (Quadrangle 5/VIII) Scale 1:250,000. Geol. Surv. Indones. Dir. Miner. Resour. Res. Dev. Centre, Bandung, Indonesia.
Sarma, D.S., Jafri, S.H., Fletcher, I.R., McNaughton, N.J., 2010. Constraints on the tectonic setting of the Andaman ophiolites, Bay of Bengal, India, from SHRIMP U–Pb zircon geochronology of plagiogranite. J. Geol. 118, 691–697.
Seton, M., Müller, R.D., Zahirovic, S., Gaina, C., Torsvik, T., Shephard, G., Talsma, A., Gurnis, M., Turner, M., Maus, S., 2012. Global continental and ocean basin reconstructions since 200 Ma. Earth-Sci. Rev. 113, 212–270.

Singh, A.K., Chung, S.-L., Bikramaditya, R.K., Lee, H.Y., 2017. New U–Pb zircon ages of plagiogranites from the Nagaland–Manipur Ophiolites, Indo-Myanmar Orogenic Belt, NE India. J. Geol. Soc. Lond. 174, 170–179.

Suwarna, N., Gafoer, S., Amin, T.C., Kusnama Hermanto, B., 1994. Geology of the Sarolangun Quadrangle. Geol. Res. Dev. Centre, Bandung, Indonesia.

Torsvik, T.H., Van der Voo, R., Preeden, U., Mac Niocaill, C., Steinberger, B., Doubrovine, P.V., van Hinsbergen, D.J.J., Domeier, M., Gaina, C., Tohver, E., 2012. Phanerozoic polar wander, palaeogeography and dynamics. Earth-Sci. Rev. 114, 325–368.

van Hinsbergen, D.J.J., Kapp, P., Dupont-Nivet, G., Lippert, P.C., DeCelles, P.G., Torsvik, T.H., 2011. Restoration of Cenozoic deformation in Asia and the size of Greater India. Tectonics 30.

van Hinsbergen, D.J.J., Lippert, P.C., Dupont-Nivet, G., McQuarrie, N., Doubrovine, P.V., Spakman, W., Torsvik, T.H., 2012. Greater India Basin hypothesis and a two-stage Cenozoic collision between India and Asia. Proc. Natl. Acad. Sci. 109, 7659–7664.

van Hinsbergen, D.J.J., Lippert, P.C., Li, S., Huang, W., Advokaat, E.L., Spakman, W., 2018. Reconstructing greater India: paleogeographic, kinematic, and geodynamic perspectives. Tectonophysics.

Velzen, A.J., van Zijderveld, J.D.A., 1995. Effects of weathering on single-domain magnetite in Early Pliocene marine marls. Geophys. J. Int. 121, 267–278.

Wajzer, M.R., Barber, A.J., Hidayat, S., 1991. Accretion, collision and strike-slip faulting: the Woyla group as a key to the tectonic evolution of North Sumatra. J. Southeast Asian Earth Sci. 6, 447–461.

Yancey, T.E., Alif, S.A., 1977. Upper Mesozoic strata near Padang, West Sumatra. Bull. Geol. Soc. Malays. 8, 61–74.

Zijderveld, J.D.A., 1967. AC demagnetization of rocks: analysis of results. In: Methods in Paleomagnetism, vol. 1, pp. 254–286.

Zwierzycki, J., 1932. Geologische Kaart van Sumatra. Schaal 1:200,000. Toelichting bij blad 2 (Kotaagoeng). D. Mijnb. Ned.